α-cluster formation and decay: The role of shell structure

Shuo Yang,[1] Chang Xu [1,*] and Gerd Röpke [2,3]

[1]*School of Physics, Nanjing University, Nanjing 210093, China*
[2]*Institut für Physik, Universität Rostock, D-18051 Rostock, Germany*
[3]*National Research Nuclear University (MEPhI), 115409 Moscow, Russia*

Shell structure effects on α-cluster formation and decay are studied by using the quartetting wave function approach (QWFA). Both the intrinsic and center-of-mass (c.o.m.) motions of an α cluster inside a core nucleus are investigated with different contributing shell model wave functions. The overlap between intrinsic wave functions of four nucleons in the α-like quartet state and in a free α particle is analyzed in detail. The change of the effective potential describing the c.o.m. motion of the quartet is explicitly shown for the major shell closures $Z = 82$ and $N = 126$. It is found that both the α-cluster formation probability and the half-life are sensitive to the quartet shell model states. By extending the QWFA calculations from ^{212}Po to α emitters with one or two extra nucleons, we show that the bound state and scattering wave functions of the α cluster are changed accordingly. The calculated α-decay half-lives agree nicely with the experimental data.

I. INTRODUCTION

One of the important subjects of nuclear theory is the exploration of the stability of nuclei. In recent years, significant progress has been made on the detection of new α emitters. The region dominated by α decay on the nuclide map has been continuously broadened owing to the rapid development of radioactive beams and new detector technology, especially in the vicinity of doubly magic nuclei. For instance, the naturally occurring ^{209}Bi was considered to be stable for a long time but was recently found to be metastable with respect to α decay [1], which makes ^{208}Pb now the heaviest stable nuclide. Very recently, the α decay of self-conjugate nucleus ^{104}Te to ^{100}Sn was successfully observed [2,3], which is the second instance of α decay to a doubly magic nucleus besides ^{212}Po. During the past several decades, much attention has been paid to the superheavy island centered near the next doubly magic nucleus (possibly ^{298}Fl), and the stability of newly synthesized superheavy nuclei is mainly determined by their α decays [4,5].

Whereas the α cluster in light nuclei has been well described by microscopic approaches [6–10], the α-cluster formation problem in heavy and superheavy nuclei has still not been fully solved although much effort has been devoted. Unlike in light nuclei, the formation of α cluster and subsequent decay process in heavy and superheavy nuclei involves a much more complex quantum many-body problem [11–29]. To perform microscopic calculations within present computer capacities, the α decays of ^{104}Te or ^{212}Po to the doubly magic core ^{100}Sn or ^{208}Pb, respectively, are of particular interest. Very recently, several studies have been devoted to a more microscopic understanding of these α decays. For example,

the proton-neutron versus α-like correlations above ^{100}Sn are investigated with an additional pocket-like surface potential simulating the four-body correlations [30]. The half-life of newly observed α decay ^{104}Te $\rightarrow$ ^{100}Sn is calculated based on energy density functionals [31]. A multistep shell model calculation is performed to analyze the α-cluster formation probabilities and subsequent decays for both ^{104}Te and ^{212}Po [32]. A larger α-cluster formation probability in nuclei above ^{100}Sn is shown when compared to analogous nuclei above ^{208}Pb [33]. A very recent review of advanced α-decay theories is provided by Mirea, in which the similarities and differences of various approaches are discussed in detail [34].

In the Wentzel-Kramers-Brillouin (WKB) type approaches of α decay, the α cluster is basically regarded as a point-like or Gaussian-like particle, which is assumed to move freely inside an effective c.o.m. potential as a whole. The decay width is determined by the c.o.m. motion of α-cluster tunneling through the Coulomb barrier. The α-cluster formation probability can be empirically extracted from experimental data [35]. In connection with the decay process, the change of the intrinsic motion between four nucleons in the α cluster is not considered in such approaches. Inspired by the pairing in nuclei and by the THSR (Tohsaki-Horiuchi-Schuck-Röpke) wave function concept [6], we recently proposed the quartetting wave function approach (QWFA) to describe α-cluster formation and decay in heavy and superheavy nuclei [36–40]. In QWFA, the motion of the four-nucleon (α-like) quartet is divided into the intrinsic motion between four nucleons within the α-like cluster and the c.o.m. motion of the α-like cluster versus the core, with a potential containing the nucleon-nucleon interaction in mean field interaction as well as the Pauli principle which is represented as a repulsion term in this effective interaction for the c.o.m. motion of the quartet [36,37]. The respective c.o.m. and intrinsic Schrödinger equations are coupled in a complex way containing derivative

*cxu@nju.edu.cn

terms of the intrinsic wave function with respect to the c.o.m. coordinate [36,37]. An important feature of α-cluster motion in QWFA is that inside the core nucleus the α cluster dissolves and four nucleons are nearly uncorrelated due to self-energy shifts and the Pauli blocking effects, which means the α cluster can only be formed on the surface of the core [38,39]. With the two-potential technique [41], the α-cluster formation probability and decay half-life can be self-consistently obtained by solving both the c.o.m. motion equation of the quartet and the scattering state of the formed α cluster [38–40].

Very recently, we improved the local density approximation of QWFA by introducing quasiparticle (shell model) nucleon states for the core nucleus and analyzed the decay properties of ideal α emitters ^{104}Te, ^{212}Po and their even-even neighbors. An improved treatment of shell structure for the core nucleus is added instead of the rigid Thomas-Fermi rule [40]. In the present work, we first investigate the intrinsic motion between four nucleons in the α cluster by taking shell structure effects into account. The overlap between the intrinsic wave functions of four nucleons in the α-like quartet state and in a free α particle is analyzed. Second, we investigate the behavior of c.o.m. effective potentials of an α cluster inside the core nucleus ^{208}Pb under the influence of different contributing shell model wave functions. In particular, we show the sensitivity of both α-cluster formation probability and half-life to different shell model states. Third, we extend the QWFA calculations from the ideal case ^{212}Po to those with one or two extra nucleons, namely, the α emitters ^{213}Po($n + {}^{212}$Po), ^{213}At($p + {}^{212}$Po), and ^{214}At($n + p + {}^{212}$Po). The influence of extra nucleons on the corresponding bound state and scattering wave functions of the quartet is analyzed and the calculated half-lives by QWFA are compared with the experimental data.

The outline of this paper is as follows. The formalism of the quartetting wave function approach is briefly given in Sec. II. In Sec. III, the intrinsic motion of four nucleons and the similarity of the intrinsic wave functions in the α-like quartet and in a free α particle are discussed. The sensitivity of α-cluster formation probability and half-life to different shell model states is discussed in Sec. IV. The numerical results of α-decay half-lives of ^{213}Po, ^{213}At, and ^{214}At are presented in Sec. V. The last section gives a short summary.

II. FORMALISM OF THE QUARTETTING WAVE FUNCTION APPROACH

Whereas the formalism of pairing, which describes two-nucleon correlations in a mean field in a self-consistent way, has been well elaborated, the description of quartetting, where the many-particle problem is approximated by considering four nucleons moving in a self-consistently determined mean field, remains a challenging problem. We focus on an α-like quartet consisting of four nucleons ($n \uparrow, n \downarrow, p \uparrow, p \downarrow$), which are implemented in the nonoccupied states above the Fermi surface of a heavy core nucleus. The interaction with this heavy core nucleus will be replaced below by an appropriately determined mean field.
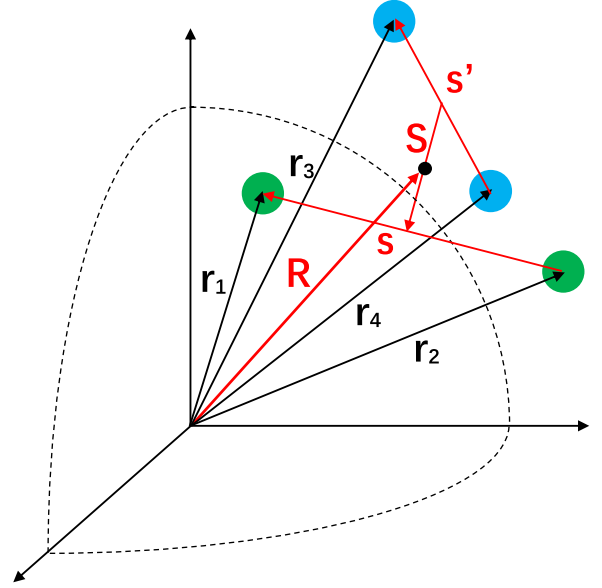
FIG. 1. A sketch of Jacobi-Moshinsky coordinates for the quartet with two protons at positions $\mathbf{r}_1 \uparrow, \mathbf{r}_2 \downarrow$ and two neutrons at positions $\mathbf{r}_3 \uparrow, \mathbf{r}_4 \downarrow$.

To calculate the wave function of this α-like quartet in position representation, we introduce a collective variable $\mathbf{R}$ describing the c.o.m. motion of the quartet, and variables that describe the intrinsic motion $\mathbf{s}_j = \mathbf{S}, \mathbf{s}, \mathbf{s}'$ with the Jacobi-Moshinsky coordinates for the quartet nucleons (see Fig. 1) [20,36,37]:

$$\mathbf{r}_1 = \mathbf{R} + \mathbf{S}/2 + \mathbf{s}/2, \quad \mathbf{r}_2 = \mathbf{R} + \mathbf{S}/2 - \mathbf{s}/2,$$
$$\mathbf{r}_3 = \mathbf{R} - \mathbf{S}/2 + \mathbf{s}'/2, \quad \mathbf{r}_4 = \mathbf{R} - \mathbf{S}/2 - \mathbf{s}'/2. \quad (1)$$

In position representation, the wave function $\Phi(\mathbf{R}, \mathbf{s}_j)$ of the quartet can be subdivided in a unique way into two normalized parts, i.e., the c.o.m. motion part $\Psi^{\mathrm{com}}(\mathbf{R})$ and the intrinsic motion part $\varphi^{\mathrm{intr}}(\mathbf{s}_j, \mathbf{R})$:

$$\Phi(\mathbf{R}, \mathbf{s}_j) = \varphi^{\mathrm{intr}}(\mathbf{s}_j, \mathbf{R})\Psi^{\mathrm{com}}(\mathbf{R}). \quad (2)$$

In particular, we are interested in the energy eigenstate of a four-nucleon Hamiltonian of the form

$$H = \left(-\frac{\hbar^2}{8m}\nabla_R^2 + T[\nabla_{s_j}]\right)\delta^3(\mathbf{R} - \mathbf{R}')\delta^3(\mathbf{s}_j - \mathbf{s}_j')$$
$$+ V(\mathbf{R}, \mathbf{s}_j; \mathbf{R}', \mathbf{s}_j') \quad (3)$$

where $-\frac{\hbar^2}{8m}\nabla_R^2$ is the kinetic energy of the c.o.m. motion and $T[\nabla_{s_j}]$ the kinetic energy of the intrinsic motion of the quartet. The interaction $V(\mathbf{R}, \mathbf{s}_j; \mathbf{R}', \mathbf{s}_j')$ contains the mutual interaction between quartet nucleons as well as the interaction of the quartet nucleons with an external potential. Below we discuss how the interaction of the quartet with the heavy core nucleus can be approximated by such an external potential. The c.o.m.

motion of the quartet satisfies the Schrödinger equation

$$
-\frac{\hbar^2}{8m}\nabla_R^2\Psi^{\mathrm{com}}(\mathbf{R}) - \frac{\hbar^2}{4m}\int d^9s_j\,\varphi^{\mathrm{intr},*}(\mathbf{s}_j,\mathbf{R})[\nabla_R\varphi^{\mathrm{intr}}(\mathbf{s}_j,\mathbf{R})]
$$
$$
\times[\nabla_R\Psi^{\mathrm{com}}(\mathbf{R})]
$$
$$
-\frac{\hbar^2}{8m}\int d^9s_j\,\varphi^{\mathrm{intr},*}(\mathbf{s}_j,\mathbf{R})\big[\nabla_R^2\varphi^{\mathrm{intr}}(\mathbf{s}_j,\mathbf{R})\big]\Psi^{\mathrm{com}}(\mathbf{R})
$$
$$
+\int d^3R'\,W(\mathbf{R},\mathbf{R}')\Psi^{\mathrm{com}}(\mathbf{R}') = E\,\Psi^{\mathrm{com}}(\mathbf{R}), \tag{4}
$$

in which $W(\mathbf{R},\mathbf{R}')$ is the nonlocal c.o.m. potential for the quartet:

$$
W(\mathbf{R},\mathbf{R}')
$$
$$
= \int d^9s_j\,d^9s'_j\,\varphi^{\mathrm{intr},*}(\mathbf{s}_j,\mathbf{R})\big[T[\nabla_{s_j}]\delta^3(\mathbf{R}-\mathbf{R}')\delta^9(\mathbf{s}_j-\mathbf{s}'_j)
$$
$$
+V(\mathbf{R},\mathbf{s}_j;\mathbf{R}',\mathbf{s}'_j)\big]\varphi^{\mathrm{intr}}(\mathbf{s}'_j,\mathbf{R}'). \tag{5}
$$

For the intrinsic motion of quartet nucleons, we have another Schrödinger equation,

$$
-\frac{\hbar^2}{4m}\Psi^{\mathrm{com},*}(\mathbf{R})[\nabla_R\Psi^{\mathrm{com}}(\mathbf{R})][\nabla_R\varphi^{\mathrm{intr}}(\mathbf{s}_j,\mathbf{R})]
$$
$$
-\frac{\hbar^2}{8m}|\Psi^{\mathrm{com}}(\mathbf{R})|^2\nabla_R^2\varphi^{\mathrm{intr}}(\mathbf{s}_j,\mathbf{R})
$$
$$
+\int d^3R'\,d^9s'_j\,\Psi^{\mathrm{com},*}(\mathbf{R})\big[T[\nabla_{s_j}]\delta^3(\mathbf{R}-\mathbf{R}')\delta^9(\mathbf{s}_j-\mathbf{s}'_j)
$$
$$
+V(\mathbf{R},\mathbf{s}_j;\mathbf{R}',\mathbf{s}'_j)\big]\Psi^{\mathrm{com}}(\mathbf{R}')\varphi^{\mathrm{intr}}(\mathbf{s}'_j,\mathbf{R}')
$$
$$
= F(\mathbf{R})\varphi^{\mathrm{intr}}(\mathbf{s}_j,\mathbf{R}). \tag{6}
$$

The Schrödinger equation of intrinsic motion is coupled with the c.o.m. motion in a rather complex way. In present calculations, the derivative terms $\nabla_R\varphi^{\mathrm{intr}}(\mathbf{s}_j,\mathbf{R})$ in Eqs. (4) and (6) are not included and a local effective c.o.m. potential $W(R)$ is introduced in order to make the calculations practical [40]. In the problem considered here, the approximation of the interaction of the quartet with the heavy core nucleus contains not only the direct nucleon-nucleon interaction [42] but also exchange terms such as the Fock self-energy and Pauli blocking, which are genuine nonlocal interactions. As shown in Sec. IV, it is possible to construct an effective local potential which reproduces the same c.o.m. wave function as $W(\mathbf{R},\mathbf{R}')$. This Pauli-blocking potential is valid in the low density region with relative error below 1% [20,36,37].

To describe the α-decay process [41], two different regions $R \leqslant R_{\mathrm{sep}}$ and $R > R_{\mathrm{sep}}$ are introduced. The effective c.o.m.

potential $W(R)$ is split into two potentials, namely the bound state potential $W_{\mathrm{bound}}(R)$ which coincides with $W(R)$ at $R \leqslant R_{\mathrm{sep}}$, and a perturbation potential $W_{\mathrm{scattering}}(R)$ which transforms the bound state to a quasistationary one. The choice of this separation radius R_{sep} does not affect the final result as long as it is large enough and ensures a bound state for the α cluster [41]. For our calculations, we take the value $R_{\mathrm{sep}} = 15$ fm. Both the bound state wave function $\Phi(R)$ of the first potential and the scattering state wave function $\chi(R)$ of the second one at R_{sep} are calculated by solving the corresponding Schrödinger equations.

As we consider that an α-like state can exist only at densities lower than the critical density $\rho_c = 0.02917$ fm^{-3} (see Refs. [20,36,37]) and dissolves at higher densities, the α-cluster preformation probability P_α can be obtained by integrating the bound state wave function $\Phi(R)$ from the critical radius R_c (where the baryon density $\rho_B(R) = \rho_c$) to infinity:

$$
P_\alpha = \int_0^\infty d^3R\,|\Phi(R)|^2\Theta[\rho_c - \rho_B(R)]. \tag{7}
$$

Approximately, for $R < R_c$, the intrinsic wave function of the quartet describes four independent nucleons in quasiparticle states (shell model), whereas the intrinsic wave function changes its character if for $R > R_c$ a bound state is formed, and becomes α-like.

The decay width given as the product of the preexponential factor ν and the exponential factor $\mathcal{T}$ is calculated by using the values of the normalized bound state wave function $\widetilde{\Phi}(R) = (4\pi)^{1/2}R\,\Phi(R)$ and the scattering wave function $\chi(R)$ at the separation radius [38,39]:

$$
\Gamma = \nu \times \mathcal{T} = \frac{4\hbar^2\zeta^2}{\mu k}|\widetilde{\Phi}(R_{\mathrm{sep}})\chi(R_{\mathrm{sep}})|^2, \tag{8}
$$

where $\mu = A_\alpha A_{\mathrm{core}}/(A_\alpha + A_{\mathrm{core}})$, $\zeta = \sqrt{2\mu[V(R_{\mathrm{sep}}) - E_{\mathrm{tunnel}}]}/\hbar$, $k = \sqrt{2\mu Q_\alpha}/\hbar$. The tunneling energy is $E_{\mathrm{tunnel}} = Q_\alpha - 28.3$ MeV, where Q_α is the experimental α decay energy. Finally the decay half-life is given by $T_{1/2} = (\hbar\ln 2)/(P_\alpha\Gamma)$.

III. INTRINSIC MOTION OF FOUR NUCLEONS AND SIMILARITY OF INTRINSIC WAVE FUNCTIONS IN QUARTET AND IN α PARTICLE

In this section, we investigate the intrinsic motion between four nucleons in the α cluster (quartet) and in a free α particle. For the latter one, its normalized intrinsic wave function may be given by the Gaussian approximation

$$
\varphi_\alpha^{\mathrm{intr}}(\mathbf{S},\mathbf{s},\mathbf{s}') = \left(\frac{a_\alpha}{\pi}\right)^{9/4}2^{-3/2}e^{-\frac{a_\alpha}{4}(2\mathbf{S}^2+\mathbf{s}^2+\mathbf{s}'^2)},
$$
$$
\text{or } \varphi_\alpha^{\mathrm{intr}}(\mathbf{r_1},\mathbf{r_2},\mathbf{r_3},\mathbf{r_4};\mathbf{R}) = \left(\frac{a_\alpha}{\pi}\right)^{9/4}2^{-3/2}e^{-\frac{a_\alpha}{2}(\mathbf{r_1^2}+\mathbf{r_2^2}+\mathbf{r_3^2}+\mathbf{r_4^2}-4\mathbf{R}^2)}
$$
$$
= \frac{\mathscr{Y}_\alpha(\mathbf{r_1})\mathscr{Y}_\alpha(\mathbf{r_2})\mathscr{Y}_\alpha(\mathbf{r_3})\mathscr{Y}_\alpha(\mathbf{r_4})}{\mathscr{Z}_\alpha(\mathbf{R})}, \tag{9}
$$

where the functions $\mathscr{Y}_\alpha(\mathbf{r}) = (a_\alpha/\pi)^{3/4} e^{-a_\alpha \mathbf{r}^2/2}$ and $\mathscr{Z}_\alpha(\mathbf{R}) = (4a_\alpha/\pi)^{3/2} e^{-4a_\alpha \mathbf{R}^2}$, respectively. The parameter $a_\alpha = 0.5351$ fm^{-2} is fitted to the rms radius ($R_{\text{rms},\alpha} = 1.45$ fm) of the α particle. According to the subdivision of the total quartet wave function into a center-of-mass (com) part and an intrinsic (intr) part [see Eq. (2)], the intrinsic wave function for the quartet is given by

$$\varphi_{\text{quartet}}^{\text{intr}}(\mathbf{R}, \mathbf{S}, \mathbf{s}, \mathbf{s}') = \frac{\Phi_{\text{quartet}}(\mathbf{R}, \mathbf{S}, \mathbf{s}, \mathbf{s}')}{\Psi_{\text{quartet}}^{\text{com}}(\mathbf{R})}, \qquad (10)$$

The total quartet wave function describes the motion of the four nucleons in a mean field produced by the remaining nucleons of the nucleus, where the antisymmetrization (i.e., the Pauli principle) of all nucleons must be satisfied. We solve this problem in two steps. In the first approximation,

we neglect the interaction between the nucleons of the quartet and approximate the mean field of the remaining nucleons by a Woods-Saxon potential widely used in shell model calculations; see the Appendix. In a second approximation, we take the interaction between the nucleons into account. The first step, where the interaction between the nucleons is only considered in mean field approximation, is solved by the shell model wave functions $R_{nl}(r) Y_{lm}(\theta, \varphi)$. We assume that inside the core of the nucleus where the nucleon density is high, these shell model wave functions give already a good description of the many-nucleon state because correlation effects are suppressed owing to Pauli blocking. Then, the total quartet wave function is approximated by the product of the constituting four shell model wave functions, and the Pauli principle is fulfilled using shell model states.

The total quartet wave function $\Phi_{\text{quartet}}(\mathbf{R}, \mathbf{S}, \mathbf{s}, \mathbf{s}')$ with the Jacobi-Moshinsky coordinates $(\mathbf{R}, \mathbf{S}, \mathbf{s}, \mathbf{s}')$ is [40]

$$\begin{aligned}
\Phi_{\text{quartet}}(\mathbf{R}, \mathbf{S}, \mathbf{s}, \mathbf{s}') = \Phi(\mathbf{r}_1, \mathbf{r}_2, \mathbf{r}_3, \mathbf{r}_4) = \sum_{J_{12}, M_{12}, J_{34}, M_{34}} \left\langle J_{12}, M_{12}, J_{34}, M_{34} \middle| J, M \right\rangle \\
\times \mathcal{A}_{12} \left\{ \sum_{m_{s1}, m_{s2}} \sum_{m_1, m_2, m_{l1}, m_{l2}} \langle j_1, m_1, j_2, m_2 | J_{12}, M_{12} \rangle \left\langle l_1, m_{l1}, \frac{1}{2}, m_{s1} \middle| j_1, m_1 \right\rangle \right. \\
\times \left. \left\langle l_2, m_{l2}, \frac{1}{2}, m_{s2} \middle| j_2, m_2 \right\rangle R_{n_1 l_1}(r) Y_{l_1 m_{l1}}(\theta_{r1}, \varphi_{r1}) R_{n_2 l_2}(r) Y_{l_2 m_{l2}}(\theta_{r2}, \varphi_{r2}) \right\} \\
\times \mathcal{A}_{34} \left\{ \sum_{m_{s3}, m_{s4}} \sum_{m_3, m_4, m_{l3}, m_{l4}} \langle j_3, m_3, j_4, m_4 | J_{34}, M_{34} \rangle \left\langle l_3, m_{l3}, \frac{1}{2}, m_{s3} \middle| j_3, m_3 \right\rangle \right. \\
\times \left. \left\langle l_4, m_{l4}, \frac{1}{2}, m_{s4} \middle| j_4, m_4 \right\rangle R_{n_3 l_3}(r) Y_{l_3 m_{l3}}(\theta_{r3}, \varphi_{r3}) R_{n_4 l_4}(r) Y_{l_4 m_{l4}}(\theta_{r4}, \varphi_{r4}) \right\},
\end{aligned} \qquad (11)$$

where $\mathcal{A}_{12}$ and $\mathcal{A}_{34}$ are antisymmetrizers and several Clebsch-Gordan coefficients are also involved (see Appendix). The notations 1,2 denote two protons $p \uparrow, p \downarrow$ in the quartet, and 3,4 denote two neutrons $n \uparrow, n \downarrow$. The quantum numbers for the total angular momentum and its z component of nucleon i are denoted by j_i and m_i, respectively. j_1 and j_2 are coupled to J_{12}, j_3 and j_4 to J_{34}, and then J_{12} and J_{34} to J. For the state of two protons or neutrons in the same orbit, J_{12} and J_{34} become zero, then we have $J_{12} = J_{34} = J = 0$, $M_{12} = M_{34} = M = 0$. Note that an example of the total quartet wave function in ^{212}Po is given in the Appendix.

The overlap between the intrinsic wave functions of quartet and α particle as a function of c.o.m. variable R can be written as

$$\begin{aligned}
\langle \varphi_\alpha^{\text{intr}} | \varphi_{\text{quartet}}^{\text{intr}} \rangle(R) &= \int d^3 S \, d^3 s \, d^3 s' \, \varphi_\alpha^{\text{intr},*}(\mathbf{S}, \mathbf{s}, \mathbf{s}') \varphi_{\text{quartet}}^{\text{intr}}(\mathbf{R}, \mathbf{S}, \mathbf{s}, \mathbf{s}') \\
&= \int d^3 S \, d^3 s \, d^3 s' \, \frac{\mathscr{Y}_\alpha^*(\mathbf{r_1}) \mathscr{Y}_\alpha^*(\mathbf{r_2}) \mathscr{Y}_\alpha^*(\mathbf{r_3}) \mathscr{Y}_\alpha^*(\mathbf{r_4}) \Phi_{\text{quartet}}(\mathbf{R}, \mathbf{S}, \mathbf{s}, \mathbf{s}')}{\mathscr{Z}_\alpha^*(\mathbf{R}) \Psi_{\text{quartet}}^{\text{com}}(\mathbf{R})} \\
&= \frac{64(2\pi)^9}{\mathscr{Z}_\alpha^*(\mathbf{R}) \Psi_{\text{quartet}}^{\text{com}}(\mathbf{R})} \int d^3 p \, \phi_{12}(\mathbf{p}) \phi_{34}(\mathbf{p}) e^{4i\mathbf{p} \cdot \mathbf{R}},
\end{aligned} \qquad (12)$$

where the c.o.m. wave function $\Psi_{\text{quartet}}^{\text{com}}(\mathbf{R})$ of the quartet can be obtained from the integral [36]

$$\Psi_{\text{quartet}}^{\text{com}}(\mathbf{R}) = \left[\int d^3 S \, d^3 s \, d^3 s' \, |\Phi_{\text{quartet}}(\mathbf{R}, \mathbf{S}, \mathbf{s}, \mathbf{s}')|^2 \right]^{1/2}. \qquad (13)$$
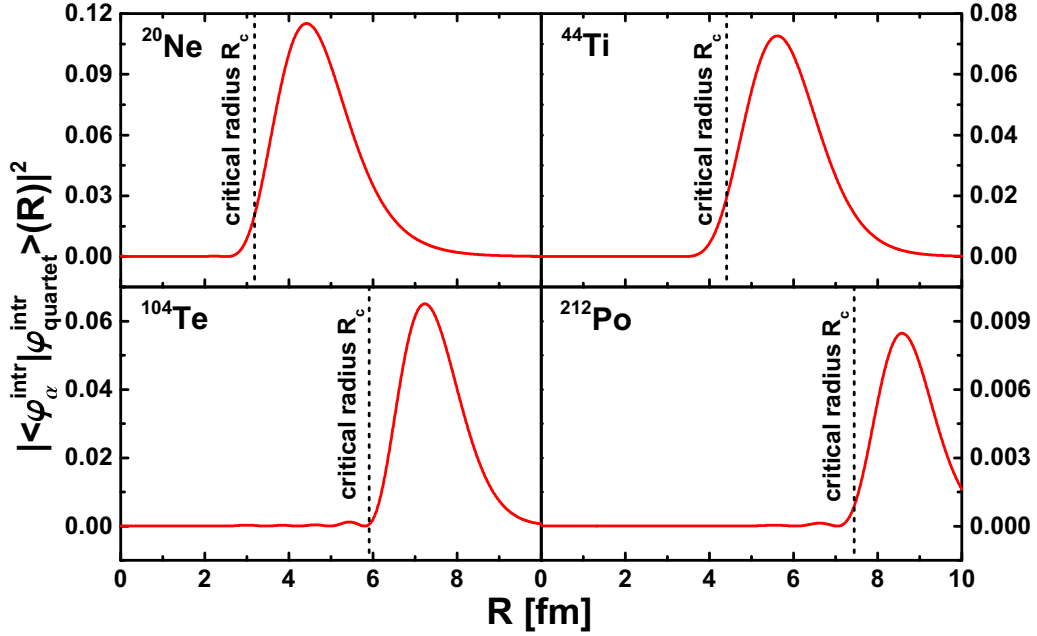
FIG. 2. The overlaps between the intrinsic wave functions of the quartet and the α-particle as a function of c.o.m. coordinate R for the α + doubly magic core systems ^{20}Ne, ^{44}Ti, ^{104}Te, and ^{212}Po.

Let $a, b = 1, 2$ or $3,4$. Then, $\phi_{ab}(\mathbf{p})$ is defined as

$$
\phi_{ab}(\mathbf{p}) = \frac{1}{(2\pi)^6} \int d^3 r_a \int d^3 r_b \mathscr{Y}_\alpha^*(\mathbf{r}_a) \mathscr{Y}_\alpha^*(\mathbf{r}_b) \Phi_{ab}(\mathbf{r}_a, \sigma_a; \mathbf{r}_b, \sigma_b) e^{-i\mathbf{p}\cdot\mathbf{r}_a - i\mathbf{p}\cdot\mathbf{r}_b}
$$

$$
= \frac{1}{(2\pi)^6} \mathcal{A}_{ab} \Bigg\{ \sum_{m_{sa}, m_{sb}} \sum_{m_a, m_b, m_{la}, m_{lb}} \langle j_a, m_a, j_b, m_b | 0, 0 \rangle \Big\langle l_a, m_{la}, \frac{1}{2}, m_{sa} \Big| j_a, m_a \Big\rangle
$$

$$
\times \Big\langle l_b, m_{lb}, \frac{1}{2}, m_{sb} \Big| j_b, m_b \Big\rangle f_{l_a, m_{la}}(\mathbf{p}) f_{l_b, m_{lb}}(\mathbf{p}) \Bigg\},
\tag{14}
$$

where the function $f_{l, m_l}(\mathbf{p})$ can be obtained from the contributing shell model wave functions

$$
f_{l, m_l}(\mathbf{p}) = \int d^3 r\, R_\alpha(r) Y_{00}^*(\theta_r, \varphi_r) R_{nl}(r) Y_{lm_l}(\theta_r, \varphi_r) e^{-i\mathbf{p}\cdot\mathbf{r}}
$$

$$
= \sqrt{4\pi} (-i)^l (2l+1) \langle l, 0, l, 0 | 0, 0 \rangle \langle l, m_l, l, -m_l | 0, 0 \rangle Y_{l\,-m_l}(\theta_p, \varphi_p)
$$

$$
\times \int_0^\infty r^2 R_{nl}(r) (\sqrt{4\pi} \mathscr{Y}_\alpha(r)) j_l(pr) dr.
\tag{15}
$$

The probability of finding the α particle in the localized shell model states can be defined as [36]

$$
\mathscr{F}_\alpha = \int dR\, 4\pi R^2 \rho_{\text{quartet}}^{\text{com}}(R) \big| \langle \varphi_\alpha^{\text{intr}} | \varphi_{\text{quartet}}^{\text{intr}} \rangle (R) \big|^2,
\tag{16}
$$

where the density $\rho_{\text{quartet}}^{\text{com}}(R) = |\Psi_{\text{quartet}}^{\text{com}}(\mathbf{R})|^2$. It is expected that the probability $\mathscr{F}_\alpha$ is small as the wave function of the quartet is approximated by a product of shell model states. It describes the character of the intrinsic wave function of the localized shell model quartet state as a function of R. The decrease at large values of R is owing to the decrease of the probability $\rho_{\text{quartet}}^{\text{com}}(R)$ of finding a quartet. In the core region, the overlap is rather small, as expected from the suppression of correlations at high densities. To identify the surface region of the nucleus, we show in Fig. 2 the value of the critical radius. Surprisingly, the intrinsic

wave function changes its shape, and in the surface region the intrinsic wave function has already nearly the form of the free α particle. In Table I, we give the numerical results of $\mathscr{F}_\alpha$ for four different groups of nuclei for comparison, namely $\{^{18}$O, ^{18}Ne, ^{20}Ne$\}$, $\{^{42}$Ca, ^{42}Ti, ^{44}Ti$\}$, $\{^{102}$Sn, ^{102}Te, ^{104}Te$\}$, and $\{^{210}$Pb, ^{210}Po, ^{212}Po$\}$. It is interesting to divide the total probability $\mathscr{F}_\alpha$ into the low density part $\mathscr{F}_\alpha^{\text{low}} = \int_{R_c}^\infty dR\, 4\pi R^2 \rho_{\text{quartet}}^{\text{com}}(R) |\langle \varphi_\alpha^{\text{intr}} | \varphi_{\text{quartet}}^{\text{intr}} \rangle (R)|^2$ and the high density one $\mathscr{F}_\alpha^{\text{high}} = \mathscr{F}_\alpha - \mathscr{F}_\alpha^{\text{low}}$. As expected, in Table I the total probability $\mathscr{F}_\alpha$ is quite small, but the low density probability $\mathscr{F}_\alpha^{\text{low}}$ is significantly enhanced for α + doubly magic core

TABLE I. Probability of finding the α-particle in the localized proton and neutron states of four groups of nuclei.

Nuclei	Proton	Neutron	$\mathscr{F}_\alpha$	$\mathscr{F}_\alpha^{low}$	$\mathscr{F}_\alpha^{low}/\mathscr{F}_\alpha$
^{18}O $(2n + {}^{16}$O$)$	$1p_{1/2}$	$1d_{5/2}$	2.239×10^{-3}	5.652×10^{-4}	0.2525
^{18}Ne $(2p + {}^{16}$O$)$	$1d_{5/2}$	$1p_{1/2}$	2.029×10^{-3}	8.743×10^{-4}	0.4309
^{20}Ne $(\alpha + {}^{16}$O$)$	$1d_{5/2}$	$1d_{5/2}$	2.004×10^{-3}	1.553×10^{-3}	0.7748
^{42}Ca $(2n + {}^{40}$Ca$)$	$1d_{3/2}$	$1f_{7/2}$	5.097×10^{-4}	8.726×10^{-5}	0.1712
^{42}Ti $(2p + {}^{40}$Ca$)$	$1f_{7/2}$	$1d_{3/2}$	4.706×10^{-4}	8.093×10^{-5}	0.1720
^{44}Ti $(\alpha + {}^{40}$Ca$)$	$1f_{7/2}$	$1f_{7/2}$	3.689×10^{-4}	1.597×10^{-4}	0.4328
^{102}Sn $(2n + {}^{100}$Sn$)$	$2p_{1/2}$	$2d_{5/2}$	1.267×10^{-4}	2.614×10^{-5}	0.2070
^{102}Te $(2p + {}^{100}$Sn$)$	$2d_{5/2}$	$2p_{1/2}$	1.074×10^{-4}	2.070×10^{-5}	0.1929
^{104}Te $(\alpha + {}^{100}$Sn$)$	$2d_{5/2}$	$2d_{5/2}$	1.316×10^{-4}	5.114×10^{-5}	0.3887
^{210}Pb $(2n + {}^{208}$Pb$)$	$3s_{1/2}$	$2g_{9/2}$	9.003×10^{-6}	3.201×10^{-6}	0.3557
^{210}Po $(2p + {}^{208}$Pb$)$	$1h_{9/2}$	$3p_{1/2}$	4.358×10^{-6}	2.323×10^{-6}	0.5332
^{212}Po $(\alpha + {}^{208}$Pb$)$	$1h_{9/2}$	$2g_{9/2}$	8.499×10^{-6}	4.810×10^{-6}	0.5660

systems ^{20}Ne, ^{44}Ti, and ^{104}Te as compared with those of their neighbors. For ^{212}Po, the quartet protons and neutrons occupy very different shell model states (see Fig. 6 in the Appendix) and their Fermi surfaces are relatively far from each other; therefore, the $\mathscr{F}_\alpha^{low}$ of ^{212}Po is slightly enhanced as compared to its neighbors. We show in Fig. 2 the overlaps between the wave functions of the quartet and the α-particle as a function of c.o.m. coordinate R for ^{20}Ne, ^{44}Ti, ^{104}Te, and ^{212}Po. It is clearly demonstrated that in each case there exists a peak in the region beyond the critical radius (i.e., the surface region of the core) [37–40]. Inside the core, the probability of finding the α-like state is quite low not only for α+core bound quantum systems ^{20}Ne and ^{44}Ti but also for open quantum systems ^{104}Te and ^{212}Po (see Fig. 2).

IV. EFFECTIVE C.O.M. POTENTIAL OF QUARTET AND SENSITIVITY OF α-DECAY HALF-LIFE TO DIFFERENT SHELL MODEL STATES

Shell structure effects manifest themselves clearly in the α-decay energy, and its value along an isotopic chain has a large gap across the major shell closures, especially the neutron one at $N = 126$. However, the gap in the α-decay energy cannot fully account for the abrupt change in the measured α-decay

half-lives. In the WKB-type approaches, the depth of the α-core effective c.o.m. potential usually needs to be shifted when crossing the $N = 126$ shell closure in order to fit the measured α-decay half-lives [17–19]. Shell structure effects also manifest themselves in the nuclear radius (or density distribution) of the core nucleus. Experiments have observed a sudden increase in the charge radius of an isotope chain (such as lead isotopes) just beyond the major shell closures [43]. Note that the calculated α-decay half-life could also be sensitive to the parametrization of nuclear radius (or density distribution) of the core.

We can construct an effective c.o.m. potential $W(R)$ which reproduces the known density $\rho_{quartet}^{com}(R)$ of the α-like cluster given by [36] according to

$$W(R) = \frac{\hbar^2}{8m} \frac{\rho_{quartet}^{com}{}'(R)}{R \rho_{quartet}^{com}(R)} - \frac{\hbar^2}{32m} \frac{\rho_{quartet}^{com}{}'(R)^2}{\rho_{quartet}^{com}(R)^2}$$
$$+ \frac{\hbar^2}{16m} \frac{\rho_{quartet}^{com}{}''(R)}{\rho_{quartet}^{com}(R)} + E. \quad (17)$$

This effective c.o.m. potential as constructed from the shell model quartet state should be nearly constant; deviations are seen in Fig. 3. At the critical radius R_c, the nucleon density falls below the critical density value $\rho_c = 0.02917$ fm^{-3} so
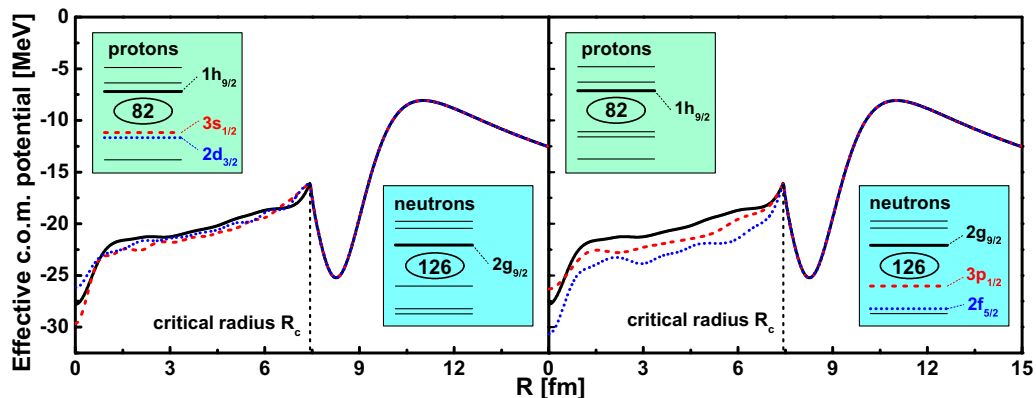
FIG. 3. The α-^{208}Pb effective c.o.m. potentials with different contributing shell model states. The sketches in the small boxes show the details of proton or neutron shell model states.
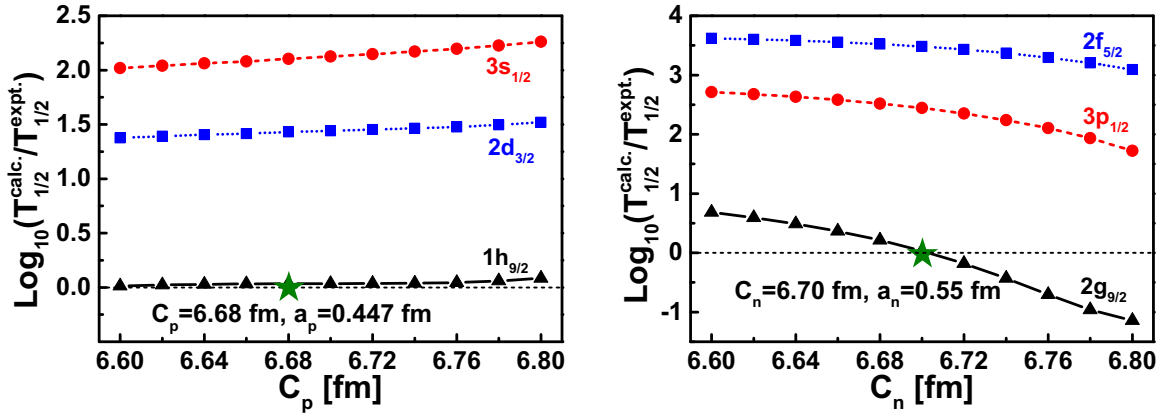
FIG. 4. The ratio of calculated α-decay half-lives to the experimental one for ^{212}Po with different contributing shell model states.

that an α cluster can be formed. We consider the second approximation where interactions between the constituents of the quartet are taken into account. In homogeneous systems, if a bound state below the continuum edge is formed, the ground-state energy is shifted by the binding energy. As described in [38–40], in the local density approximation we use the density dependent shift of the α particle for the intrinsic energy shift $E(R)$, which takes the value -28.3 MeV in the limit of large R.

In Fig. 3, we show in left panel the c.o.m. effective potentials of an α cluster in ^{208}Pb constructed with three different quartet proton states $1h_{9/2}$, $3s_{1/2}$, and $2d_{3/2}$, and in right panel with three different quartet neutron states $2g_{9/2}$, $3p_{1/2}$, and $2f_{5/2}$. It is shown that the "pocket" in the surface region is still formed after introducing different shell model states for the quartet nucleons. Sharp edges at the critical radius R_c can be avoided in future with a better account of gradient effects. In the core region, the effective c.o.m. potential reveals a moderate shift for the $Z = 82$ shell closure, but a very large one for the $N = 126$ shell closure (see the right panel). So the c.o.m. effective potential $W(R)$ is rather sensitive to the details of contributing neutron states, and the impact of the change of $W(R)$ on both the α-cluster formation probability and half-life cannot be neglected.

As introduced in our previous work [40], for the density distribution of protons and neutrons, we use the parametrized Fermi functions $\rho_p(R) = \rho_{p0}/[1 + e^{(R-C_p)/a_p}]$, $\rho_n(R) = \rho_{n0}/[1 + e^{(R-C_n)/a_n}]$ where C_p, C_n are the half-density radii and a_p, a_n are the diffuseness parameters for protons and neutrons. For the core nucleus ^{208}Pb, the parametrization of the density distribution is constrained by both the electron scattering and coherent pion photoproduction data, i.e., $C_p = 6.68$ fm, $C_n = 6.70$ fm, $a_p = 0.447$ fm, $a_n = 0.55$ fm [44]. For the purpose of comparison, we change the half-density radii C_p and C_n in a reasonable range, from 6.60 to 6.80 fm, in our analysis. The corresponding a_p and a_n are obtained by the following relation with the rms radius unchanged [45].

$$a = \sqrt{\frac{5}{7\pi^2}\left(\langle r^2 \rangle - \frac{3}{5}C^2\right)}. \quad (18)$$

Figure 4 gives the ratio of calculated α-decay half-life to the experimental one for ^{212}Po as a function of half-density radii C_p (left panel) and C_n (right panel). The star symbol denotes the reference result, in which both the "correct" density distributions and "correct" quartet states are applied. It is shown in Fig. 4 that there is substantial change in the α-decay half-life by using different quartet states. For instance, the
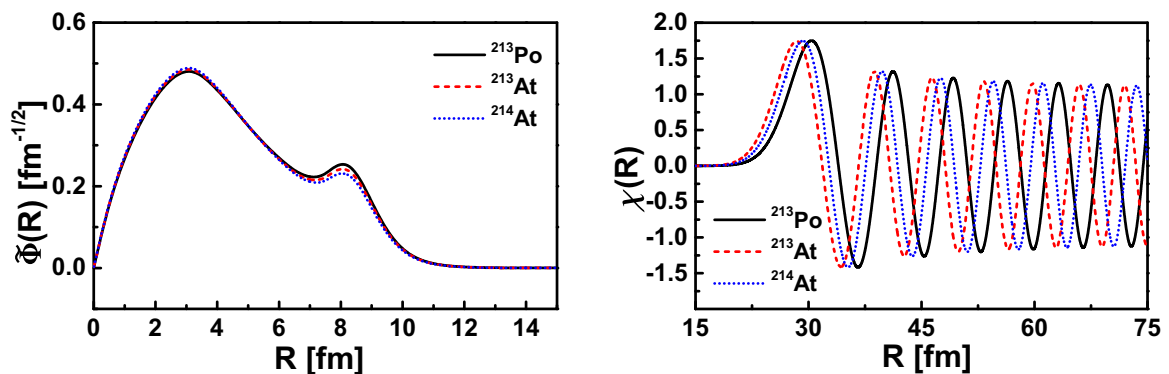
FIG. 5. The bound state wave functions and scattering wave functions for α emitters ^{213}Po, ^{213}At, and ^{214}At in the two-potential approach. The separating radius is chosen to be $R_{\text{sep}} = 15$ fm. In the left panel, the normalized bound state wave function $\widetilde{\Phi}(R) = (4\pi)^{1/2}R\Phi(R)$, $\int_0^\infty |\widetilde{\Phi}(R)|^2 dR = 1$ is shown.

TABLE II. The QWFA calculations of the α-cluster formation probabilities and half-lives for ^{213}Po, ^{213}At, and ^{214}At.

Parent	I^π	proton	neutron	Q_α (MeV)	P_α	$T_{1/2}^{\text{expt.}}$ (s)	$T_{1/2}^{\text{calc.}}$ (s)
^{213}Po(^{212}Po $+n$)	$\frac{9}{2}^+ \to \frac{9}{2}^+$	$1h_{9/2}$	$2g_{9/2}$	8.537	0.0952	4.200×10^{-6}	3.160×10^{-6}
^{213}At(^{212}Po $+p$)	$\frac{9}{2}^- \to \frac{9}{2}^-$	$1h_{9/2}$	$2g_{9/2}$	9.254	0.1021	1.250×10^{-7}	1.626×10^{-7}
^{214}At(^{212}Po $+n+p$)	$1^- \to 1^-$	$1h_{9/2}$	$2g_{9/2}$	8.987	0.0928	5.639×10^{-7}	6.865×10^{-7}

α-decay half-life can be altered by more than three orders of magnitude by changing the quartet neutron state from $2f_{5/2}$ to $2g_{9/2}$. Interestingly, the calculated α-decay half-life is found to be more sensitive to the neutron half-density radius C_n than the proton one C_p. This is probably because the Coulomb potential/barrier changes with the proton half-density radius C_p as well.

V. EXTENSION OF QWFA CALCULATIONS TO ODD-A α EMITTERS ^{213}Po, ^{213}At AND ODD-ODD ONE ^{214}At

Now we extend the QWFA calculation to the cases with one or two extra nucleons added to the ideal α emitter ^{212}Po, i.e., ^{213}Po($n + ^{212}$Po), ^{213}At($p + ^{212}$Po), and ^{214}At($n + p + ^{212}$Po). We analyze the influence of the extra nucleons on both the bound state wave function and scattering wave function of the α-cluster. Because the ground-state to ground-state transitions of these α emitters are favored and the branching ratios are almost 100%, we assume that the angular momentum carried away by the α particle is zero and other decay channels are not involved. The problem of partially filled shells is not considered here, which should be included when spherical symmetry can no longer be assumed. The information of the core radius is not complete, especially the neutron radius, so we make a simple extrapolation of the density distribution of ^{208}Pb. A Fermi function is still used for the density distribution of core nucleus, in which the half-density radii are $C_p = 1.538 Z_d^{1/3}$ fm and $C_n = 1.336 N_d^{1/3}$ fm, respectively. The parameters 1.538 and 1.336 are obtained directly by fitting the experimental half-density radii of ^{208}Pb [44]. Z_d and N_d are the proton number and the neutron number of the core nucleus, respectively. The diffuseness parameters of both protons and neutrons are kept the same, $a_p = 0.447$ fm and $a_n = 0.55$ fm [44]. For these α emitters, the extra proton occupies the same $1h_{9/2}$ state as the quartet protons and extra neutron the same $2g_{9/2}$ state as the quartet neutrons.

Both the bound state and scattering state wave functions of the α cluster for ^{213}Po, ^{213}At, and ^{214}At are plotted in Fig. 5. The behavior of the bound state wave functions $\widetilde{\Phi}(R)$ for these α emitters is rather similar in the inner region. In the outside region, a small peak of the bound state wave function around $R = 8$ fm is clearly shown in Fig. 5, as a result of the "pocket" in the effective c.o.m. potential. The scattering state wave functions in Fig. 5 show an oscillating feature with different phase shifts due to different decay energies. The numerical results of QWFA for ^{213}Po, ^{213}At, and ^{214}At are summarized in Table II. It is seen that the α-cluster formation probabilities of these nuclei are close to each other, but slightly smaller than that of even-even α emitter ^{212}Po ($P_\alpha = 0.1045$). This feature, associated with the blocking effect of an extra nucleon, is consistent with a previous empirical analysis of α-decay data [18].

Surprisingly, it is seen from Table II that the experimental α-decay half-lives (see Ref. [46]) are reproduced quite nicely without fitting any parameter in QWFA.

VI. SUMMARY

By using the quartetting wave function approach, both the intrinsic and c.o.m. motions of the α-like cluster inside the core nucleus are investigated under the influence of different contributing shell model wave functions. We found from the intrinsic motions that the probability of finding the α particle in the localized shell model states is enhanced for the $\alpha +$ doubly magic core systems as compared to their neighbors containing additional nucleons. The overlap between the intrinsic wave functions of the α-like cluster and the free α particle shows that the α-like state can be formed on the surface of the core nucleus. We also found from the c.o.m. motions that the shell structure effects result in an abrupt shift of the α-core effective potentials across the major shell closures. The α-decay half-life is quite sensitive to different contributing quartet shell model states. We further extend the
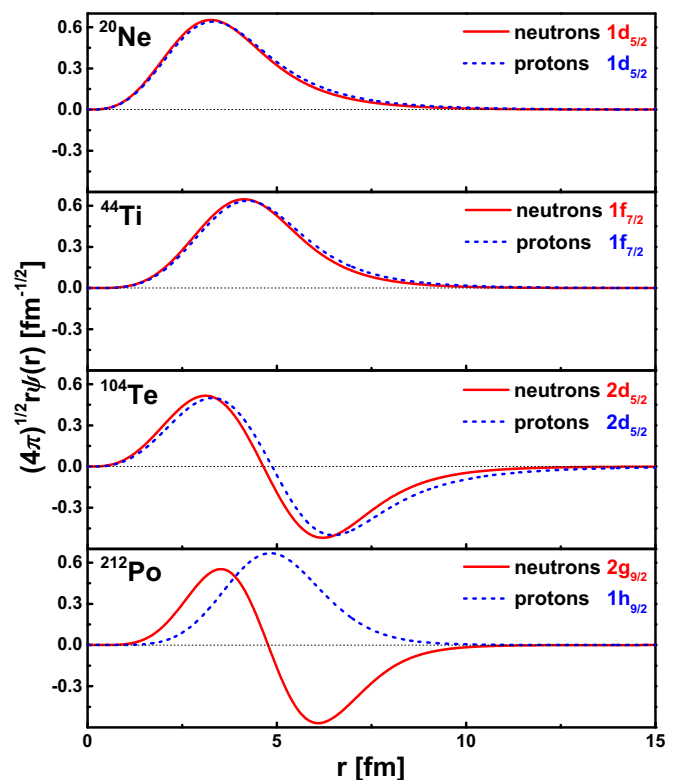
FIG. 6. The contributing single-particle wave functions of protons and neutrons in the quartets of ^{20}Ne, ^{44}Ti, ^{104}Te, and ^{212}Po.

QWFA calculations to the α emitters with one or two extra nucleons. The calculated α-decay half-lives are found to be in excellent agreement with the experimental data.

APPENDIX: SHELL MODEL WAVE FUNCTIONS WITH THE WOODS-SAXON POTENTIAL

In present calculations, we use the widely used Woods-Saxon potential

$$V_{\text{WS}}(r) = \frac{V_0}{1 + \exp\left(\frac{r-R_0}{a}\right)} \tag{A1}$$

together with the spin-orbit coupling interaction

$$V_{\text{so}}(r) = \frac{1}{2\mu^2 r}\left(\frac{\partial}{\partial r}\frac{\lambda V_0}{1 + \exp(\frac{r-R_{\text{so}}}{a_{\text{so}}})}\right)\mathbf{l}\cdot\mathbf{s} \tag{A2}$$

to determine the shell model wave functions of quartet nucleons. The strength of the Woods-Saxon potential is parametrized as $V_0 = -46[1 \pm 0.97(\frac{N-Z}{A})]$ ("+" for protons and "−" for neutrons). The parameter R_0 is $1.43A^{1/3}$ fm for both protons and neutrons while the parameter R_{so} is $1.37A^{1/3}$ fm. The diffusivity parameters a and a_{so} are chosen to be the same value 0.7 fm. μ is the reduced mass of the α-core system and the normalization factor of the ls coupling strength λ is 37.5 for neutrons and 31 for protons, respectively. The Coulomb potential we adopt is

$$V_C(r) = (Z-1)e^2\begin{cases}(3R_{\text{Coul}}^2 - r^2)/2R_{\text{Coul}}^3, & r \leqslant R_{\text{Coul}}, \\ 1/r, & r > R_{\text{Coul}},\end{cases} \tag{A3}$$

with the radius $R_{\text{Coul}} = 1.25A^{1/3}$ fm. Note that all the parameters for the Woods-Saxon potential and the ls coupling remain the same as those in our previous work [40]. We show in Fig. 6 the shell model wave functions of quartet nucleons for ^{20}Ne, ^{44}Ti, ^{104}Te, and ^{212}Po, respectively. It is clearly seen that, for ^{20}Ne, ^{44}Ti, ^{104}Te, the shell model wave functions for quartet protons and quartet neutrons are almost identical. For ^{212}Po, the proton wave function $1h_{9/2}$ is quite different from the neutron one $2g_{9/2}$. The total wave function for the quartet $\Phi_{\text{quartet}}(\mathbf{R}, \mathbf{S}, \mathbf{s}, \mathbf{s}')$ in ^{212}Po can be given by

$$\Phi_{\text{quartet}}(\mathbf{R}, \mathbf{S}, \mathbf{s}, \mathbf{s}') = \Phi_{\text{quartet}}(\mathbf{r}_1, \mathbf{r}_2, \mathbf{r}_3, \mathbf{r}_4)$$

$$= \left[\frac{\sqrt{2}}{2}\left(\sum_{m_1=-\frac{9}{2}}^{\frac{9}{2}}\left\langle\frac{9}{2}, m_1, \frac{9}{2}, -m_1\Big|0, 0\right\rangle\left\langle 5, m_1 - \frac{1}{2}, \frac{1}{2}, \frac{1}{2}\Big|\frac{9}{2}, m_1\right\rangle\right.\right.$$

$$\times\left\langle 5, -m_1 + \frac{1}{2}, \frac{1}{2}, -\frac{1}{2}\Big|\frac{9}{2}, -m_1\right\rangle\sqrt{4\pi}\psi_p(r_1)Y_{5,m_1-\frac{1}{2}}(\theta_{r1}, \varphi_{r1})$$

$$\times\sqrt{4\pi}\psi_p(r_2)Y_{5,-m_1+\frac{1}{2}}(\theta_{r2}, \varphi_{r2})\right) - \frac{\sqrt{2}}{2}\left(\sum_{m_1=-\frac{9}{2}}^{\frac{9}{2}}\left\langle\frac{9}{2}, m_1, \frac{9}{2}, -m_1\Big|0, 0\right\rangle\right.$$

$$\times\left\langle 5, m_1 + \frac{1}{2}, \frac{1}{2}, -\frac{1}{2}\Big|\frac{9}{2}, m_1\right\rangle\left\langle 5, -m_1 - \frac{1}{2}, \frac{1}{2}, \frac{1}{2}\Big|\frac{9}{2}, -m_1\right\rangle$$

$$\times\sqrt{4\pi}\psi_p(r_1)Y_{5,m_1+\frac{1}{2}}(\theta_{r1}, \varphi_{r1})\sqrt{4\pi}\psi_p(r_2)Y_{5,-m_1-\frac{1}{2}}(\theta_{r2}, \varphi_{r2})\right)\right]$$

$$\times\left[\frac{\sqrt{2}}{2}\left(\sum_{m_3=-\frac{9}{2}}^{\frac{9}{2}}\left\langle\frac{9}{2}, m_3, \frac{9}{2}, -m_3\Big|0, 0\right\rangle\left\langle 4, m_3 - \frac{1}{2}, \frac{1}{2}, \frac{1}{2}\Big|\frac{9}{2}, m_3\right\rangle\right.\right.$$

$$\times\left\langle 4, -m_3 + \frac{1}{2}, \frac{1}{2}, -\frac{1}{2}\Big|\frac{9}{2}, -m_3\right\rangle\sqrt{4\pi}\psi_n(r_3)Y_{4,m_3-\frac{1}{2}}(\theta_{r3}, \varphi_{r3})$$

$$\times\sqrt{4\pi}\psi_n(r_4)Y_{4,-m_3+\frac{1}{2}}(\theta_{r4}, \varphi_{r4})\right) - \frac{\sqrt{2}}{2}\left(\sum_{m_3=-\frac{9}{2}}^{\frac{9}{2}}\left\langle\frac{9}{2}, m_3, \frac{9}{2}, -m_3\Big|0, 0\right\rangle\right.$$

$$\times\left\langle 4, m_3 + \frac{1}{2}, \frac{1}{2}, -\frac{1}{2}\Big|\frac{9}{2}, m_3\right\rangle\left\langle 4, -m_3 - \frac{1}{2}, \frac{1}{2}, \frac{1}{2}\Big|\frac{9}{2}, -m_3\right\rangle$$

$$\times\sqrt{4\pi}\psi_n(r_3)Y_{4,m_3+\frac{1}{2}}(\theta_{r3}, \varphi_{r3})\sqrt{4\pi}\psi_n(r_4)Y_{4,-m_3-\frac{1}{2}}(\theta_{r4}, \varphi_{r4})\right)\right], \tag{A4}$$

where the Clebsch-Gordan coefficients can be found in Ref. [47].

[1] P. de Marcillac, N. Coron, G. Dambier, J. Leblanc, and J. P. Moalic, Nature (London) **422**, 876 (2003).

[2] K. Auranen, D. Seweryniak, M. Albers, A. D. Ayangeakaa, S. Bottoni, M. P. Carpenter, C. J. Chiara, P. Copp, H. M. David, D. T. Doherty, J. Harker, C. R. Hoffman, R. V. F. Janssens, T. L. Khoo, S. A. Kuvin, T. Lauritsen, G. Lotay, A. M. Rogers, J. Sethi, C. Scholey, R. Talwar, W. B. Walters, P. J. Woods, and S. Zhu, Phys. Rev. Lett. **121**, 182501 (2018).

[3] Y. Xiao, S. Go, R. Grzywacz, R. Orlandi, A. N. Andreyev, M. Asai, M. A. Bentley, G. de Angelis, C. J. Gross, P. Hausladen, K. Hirose, S. Hofmann, H. Ikezoe, D. G. Jenkins, B. Kindler, R. Léguillon, B. Lommel, H. Makii, C. Mazzocchi, K. Nishio, P. Parkhurst, S. V. Paulauskas, C. M. Petrache, K. P. Rykaczewski, T. K. Sato, J. Smallcombe, A. Toyoshima, K. Tsukada, K. Vaigneur, and R. Wadsworth, Phys. Rev. C **100**, 034315 (2019).

[4] Y. T. Oganessian, A. Sobiczewski, and G. M. Ter-Akopian, Phys. Scr. **92**, 023003 (2017).

[5] J. H. Hamilton, S. Hofmann, and Y. T. Oganessian, Annu. Rev. Nucl. Part. Sci. **63**, 383 (2013).

[6] A. Tohsaki, H. Horiuchi, P. Schuck, and G. Röpke, Phys. Rev. Lett. **87**, 192501 (2001).

[7] J. A. Wheeler, Phys. Rev. **52**, 1083 (1937).

[8] D. L. Hill and J. A. Wheeler, Phys. Rev. **89**, 1102 (1953).

[9] M. Chernykh, H. Feldmeier, T. Neff, P. von Neumann-Cosel, and A. Richter, Phys. Rev. Lett. **98**, 032501 (2007) and references therein.

[10] Y. Kanada-En'yo, Progr. Theor. Phys. **117**, 655 (2007) and references therein.

[11] H. J. Mang, Phys. Rev **119**, 1069 (1960).

[12] K. Varga, R. G. Lovas, and R. J. Liotta, Phys. Rev. Lett. **69**, 37 (1992).

[13] D. S. Delion, R. J. Liotta, and R. Wyss, Phys. Rev. C **92**, 051301(R) (2015).

[14] V. Yu. Denisov and A. A. Khudenko, Phys. Rev. C **79**, 054614 (2009).

[15] B. A. Brown, Phys. Rev. C **46**, 811 (1992).

[16] Y. Hatsukawa, H. Nakahara, and D. C. Hoffman, Phys. Rev. C **42**, 674 (1990).

[17] B. Buck, A. C. Merchant, and S. M. Perez, Phys. Rev. C **45**, 2247 (1992).

[18] C. Xu and Z. Ren, Phys. Rev. C **74**, 014304 (2006).

[19] P. Mohr, Phys. Rev. C **73**, 031301(R) (2006).

[20] G. Röpke, P. Schuck, Y. Funaki, H. Horiuchi, Zhongzhou Ren, A. Tohsaki, Chang Xu, T. Yamada, and Bo Zhou, Phys. Rev. C **90**, 034304 (2014).

[21] R. G. Lovas, R. J. Liotta, A. Insolia, K. Varga, and D. S. Delion, Phys. Rep. **294**, 265 (1998).

[22] D. S. Delion, R. J. Liotta, and R. Wyss, Phys. Rep. **424**, 113 (2006).

[23] C. Qi, R. J. Liotta, and R. Wyss, Prog. Part. Nucl. Phys. **105**, 214 (2019).

[24] J. M. Dong, Q. Zhao, L. J. Wang, W. Zuo, and J. Z. Gu, Phys. Lett. B **813**, 136063 (2021).

[25] Y. Taniguchi, K. Yoshida, Y. Chiba, Y. Kanada-En'yo, M. Kimura, and K. Ogata, Phys. Rev. C **103**, L031305 (2021).

[26] E. Nakano, K. Iida, and W. Horiuchi, Phys. Rev. C **102**, 055802 (2020).

[27] M. Ismail, W. M. Seif, and A. Abdurrahman, Phys. Rev. C **94**, 024316 (2016).

[28] J. G. Deng, H. F. Zhang, and G. Royer, Phys. Rev. C **101**, 034307 (2020).

[29] J. E. Perez Velasquez, N. G. Kelkar, and N. J. Upadhyay, Phys. Rev. C **99**, 024308 (2019).

[30] V. V. Baran and D. S. Delion, Phys. Rev. C **94**, 034319 (2016).

[31] F. Mercier, J. Zhao, R. D. Lasseri, J. P. Ebran, E. Khan, T. Nikšić, and D. Vretena, Phys. Rev. C **102**, 011301(R) (2020).

[32] M. Patial, R. J. Liotta, and R. Wyss, Phys. Rev. C **93**, 054326 (2016).

[33] R. M. Clark, A. O. Macchiavelli, H. L. Crawford, P. Fallon, D. Rudolph, A. Såmark-Roth, C. M. Campbell, M. Cromaz, C. Morse, and C. Santamaria, Phys. Rev. C **101**, 034313 (2020).

[34] M. Mirea, Eur. Phys. J. A **56**, 151 (2020).

[35] J. C. Batchelder, K. S. Toth, C. R. Bingham, L. T. Brown, L. F. Conticchio, C. N. Davids, D. Seweryniak, J. Wauters, J. L. Wood, and E. F. Zganjar, Phys. Rev. C **55**, R2142(R) (1997).

[36] G. Röpke, P. Schuck, C. Xu, Z. Ren, M. Lyu, B. Zhou, Y. Funaki, H. Horiuchi, A. Tohsaki, and T. Yamada, J. Low Temp. Phys. **189**, 383 (2017).

[37] G. Röpke, in *Proceedings of the 4th International Workshop on "State of the Art in Nuclear Cluster Physics" (SOTANCP4), 13–18 May 2018*, Texas, edited by M. Barbui, C. M. Folden, III, V. Z. Goldberg, and G. V. Rogachev, AIP Conf Proc. No. 2038 (AIP, New York, 2018), p. 020008.

[38] C. Xu, Z. Ren, G. Röpke, P. Schuck, Y. Funaki, H. Horiuchi, A. Tohsaki, T. Yamada, and B. Zhou, Phys. Rev. C **93**, 011306(R) (2016).

[39] C. Xu, G. Röpke, P. Schuck, Z. Ren, Y. Funaki, H. Horiuchi, A. Tohsaki, T. Yamada, and Bo Zhou, Phys. Rev. C **95**, 061306(R) (2017).

[40] S. Yang, C. Xu, G. Röpke, P. Schuck, Z. Ren, Y. Funaki, H. Horiuchi, A. Tohsaki, T. Yamada, and B. Zhou, Phys. Rev. C **101**, 024316 (2020).

[41] S. A. Gurvitz, Phys. Rev. A **38**, 1747 (1988); S. A. Gurvitz and G. Kalbermann, Phys. Rev. Lett. **59**, 262 (1987).

[42] G. R. Satchler and W. G. Love, Phys. Rep. **55**, 183 (1979).

[43] I. Angeli and K. P. Marinova, At. Data Nucl. Data Tables **99**, 69 (2013).

[44] C. M. Tarbert *et al.*, Phys. Rev. Lett. **112**, 242502 (2014).

[45] M. Warda, X. Viñas, X. Roca-Maza, and M. Centelles, Phys. Rev. C **81**, 054309 (2010).

[46] G. Audi, F. G. Kondev, M. Wang, W. J. Huang, and S. Naimi, Chin. Phys. C **41**, 030001 (2017).

[47] M. E. Rose, *Elementary Theory of Angular Momentum* (Dover, New York, 1995).